Research Square

Preprints are preliminary reports that have not undergone peer review.
They should not be considered conclusive, used to inform clinical practice,
or referenced by the media as validated information.

Effect of Easily Reducible Iron(III) Complexes with Trihydroxamate-Type Artificial Siderophores on Iron-Uptake Mechanisms to the Siderophore-Auxotrophic Gram-Positive Bacterium Microbacterium flavescens

Kenji Matsumoto
Kochi University
Tomohiro Ozawa
Nagoya Institute of Technology
Tomohiko Inomata
Nagoya Institute of Technology
Hideki Masuda
hidekimasuda@yahoo.co.jp

Suzuka University of Medical Science

Research Article

Keywords: Artificial siderophore, Hydroxamic acid, Iron transport process, Reductive process, Microbacterium, flavescens

Posted Date: November 24th, 2026

DOI: https://doi.org/10.21203/rs.3.rs-11038748/v1

License: This work is licensed under a Creative Commons Attribution 4.0 International License.
Read Full License

Additional Declarations: No competing interests reported.

Effect of Easily Reducible Iron(III) Complexes with Trihydroxamate-Type Artificial Siderophores on Iron-Uptake Mechanisms to the Siderophore-Auxotrophic Gram-Positive Bacterium *Microbacterium flavescens*

Kenji Matsumoto,[a] Tomohiro Ozawa,[b] Tomohiko Inomata,[b] and Hideki Masuda*[b,c]

[a] Professor/Dr. K. Matsumoto
Department of Chemistry and Biotechnology, Faculty of Science and Technology
Kochi University
2-5-1 Akebono-cho, Kochi 780-8520, Japan

[b] Professors/Drs. T. Ozawa, T. Inomata and H. Masuda
Graduate School of Engineering
Nagoya Institute of Technology
Gokiso-cho, Showa-ku, Nagoya 466-8555, Japan

[c] Professor/Dr. H. Masuda
Faculty of Pharmaceutical Sciences
Suzuka University of Medical Science
3500-1 Tamagaki-cho, Suzuka 513-8670, Japan
E-mail: hidekimasuda@yahoo.co.jp

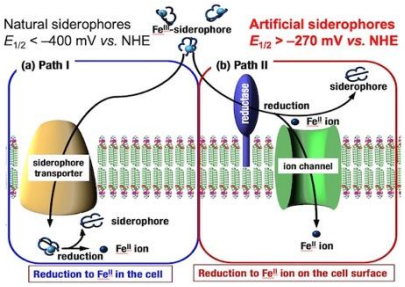
Abstract

The electrochemical properties of Fe(III) complexes of TAGE and TAGP synthesized as hydroxamate-type artificial siderophores were investigated. They present high redox potentials of $E_{1/2}$ = −227 and −268 mV vs. NHE, respectively, which are 150 to 250 mV higher than natural hydroxamate-type siderophore Fe(III) complexes. Consequently, the artificial siderophore Fe(III)-TAGE is reduced by ascorbic acid to release Fe(II) ions, whereas the natural siderophore Fe(III)-DFOB is not reduced, consistent with their respective electrochemical behaviors. Using these artificial Fe(III) siderophore complexes,

the bioavailability of *Microbacterium flavescens* was investigated. It has long been believed that its iron uptake mechanism depends solely on the direct uptake of Fe(III) hydroxamate-type siderophores. The growth behaviors of *M. flavescens* in response to these siderophores were examined in the presence and absence of 2,2'-bipyridine (Bpy), an Fe(II) chelator. The artificial siderophore Fe(III) complexes promote the growth of *M. flavescens* in the absence of Bpy, as do natural siderophores. However, the artificial siderophores did not promote growth in the presence of Bpy. This suggests that the Fe(III) ions in the artificial siderophore complexes are reduced to Fe(II) ions and that the less stable Fe(II) ions are captured by Bpy, preventing the growth of *M. flavescens*. These results suggest that *M. flavescens* also possesses a reductive iron transport pathway.

Graphical Abstracts

Artificial Fe(III) siderophores exhibit significantly higher reduction potentials than natural ones do. In biological assays using the auxotroph *Microbacterium flavescens*, the addition of an extracellular Fe(II) chelator selectively inhibited growth exclusively for these artificial complexes. These findings indicate that iron is reduced prior to uptake, suggesting that this bacterium possesses an alternative reductive iron transport pathway.

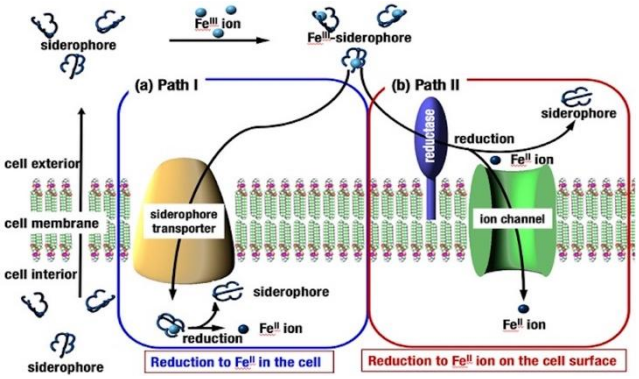


Keywords. Artificial siderophore • Hydroxamic acid • Iron transport process • Reductive process • *Microbacterium. flavescens*

Introduction

Iron is one of the most essential elements for living things because most of them require iron to maintain their life [1–10]. Recently, it has been shown that iron effectively promotes the growth of plants, which leads to a reduction in CO_2 and increased productivity [11–13]. Since it is very difficult for organisms to obtain iron due to the low solubility (approximately 10^{-18} M) of Fe(III) ions at physiological pH (pH 7), microorganisms and plants take up iron ions into the cell interior via chelated compounds called siderophores via the following processes [1–10]. Siderophores are synthesized intracellularly and released

extracellularly to capture iron ions from the environment as a stable siderophore Fe(III) complex, and they are then taken up by the cell primarily through the following two pathways: Path I, which is an intact uptake process in which an Fe(III) siderophore complex is transported into a cell interior *via* membrane-associated transporter systems (Scheme 1(a)) [4–10, 14–17]. Path II is a reductive process in which an iron ion is directly transported into the cell interior *via* an ion channel after the reduction of Fe(III) siderophore complexes to Fe(II) species by membrane-bound or extracellular reductases and photolysis (Scheme 1(b)) [4–10,14–17]. Path I has been found in various gram-negative bacteria and fungi and has been characterized by crystal structure analyses of transporter proteins and many mutational experiments [4–6]. Path II is predominantly found in yeasts, phytoplanktons and plants [11–13,15,17]. Unlike gram-negative bacteria, gram-positive bacteria lack an outer membrane. Therefore, their iron uptake is relatively straightforward and directly relies on siderophore-receptor proteins and ATP-binding cassette (ABC) transporters on the cytoplasmic membrane [18,19]. In addition, some gram-positive bacteria also have other iron uptake systems [20-22].

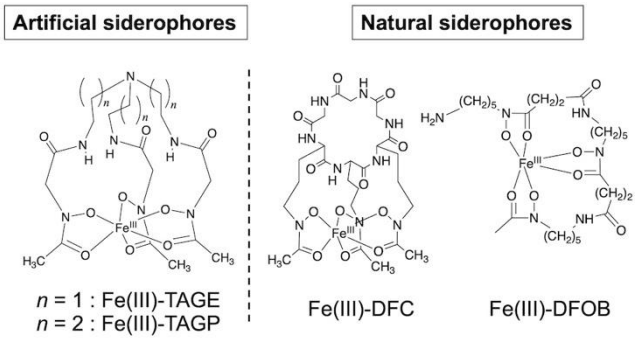


Scheme 1. Mechanism of iron ion transport into cells by (a) Path I *via* siderophore transporters and (b) Path II *via* ion channels in microorganisms.

Previously, we synthesized an artificial siderophore Fe(III) complex containing a hydroxamic acid group as a structural model of the natural siderophores deferriferrichrome (DFC) (Scheme 2), tris[2-{(*N*-acetyl-κ*O*-*N*-oxo-κ*O*)aminomethylamido}ethyl]amine iron (III) (Fe(III)-TAGE) and tris[3-{(*N*-acetyl-κ*O*-*N*-oxo-κ*O*)aminomethylamido}propyl]amine iron(III) (Fe(III)-TAGP), investigated their structural characteristics, stability, and bioavailability [23–25]. Although TAGE has a structural feature similar to that of the natural siderophore DFC, the redox potential of its Fe(III) complex, Fe(III)-TAGE ($E_{1/2}$ = –230 mV *vs* NHE) [23], has a higher redox potential than the Fe(III) complexes of trihydroxamate-type natural siderophores, Fe(III)-DFC ($E_{1/2}$ = –392 mV *vs* NHE) [26] and Fe(III)-DFOB (desferrioxamine B) ($E_{1/2}$ = –482 mV *vs* NHE) [27]. We believe that this is due to the hydrogen bonding interaction between the NH group of the artificial siderophore and the carbonyl oxygen of the hydroxamic acid group. Furthermore, we also examined the biological activity of Fe(III)-TAGE in *Microbacterium flavescens* (*M. flavescens*, ATCC No. 25091 [28,29]). This is because *M. flavescens* is a gram-positive bacterium that lacks the ability to produce its own siderophores and therefore

requires hydroxamate-type siderophores for growth. Fortunately, Fe(III)-TAGE promoted the growth of *M. flavescens*. Fe(III)-TAGP also promoted the growth of this bacterium, although the redox potential had not yet been measured. Since it is believed that *M. flavescens* possesses only one pathway (Path I) that utilizes Fe(III)-hydroxamate-type siderophores as an iron source, this bacterium has primarily been used to investigate the bioavailability of artificial hydroxamate-type siderophores [28,29]. Consequently, we initially assumed that Fe(III)-TAGE and Fe(III)-TAGP would be taken up by *M. flavescens* cells *via* Path I. However, through subsequent further investigations, we became aware that *M. flavescens* may have iron transport pathways other than Path I.

In this study, we reexamined the cyclic voltammetry (CV) of Fe(III)-TAGE and reevaluated its growth-promoting effect on *M. flavescens* when it was used in combination with Fe(III)-TAGP. In particular, using these artificial siderophores, we observed the growth behavior of *M. flavescens* in the presence and absence of 2,2'-bipyridine (Bpy). These results revealed that, in addition to Path I, the pathway by which *M. flavescens* takes up Fe(III)-siderophore complexes as they are, an alternative iron uptake pathway, Path II, which proceeds *via* iron reduction, exists. Here, we report on this approach and the findings obtained.



Scheme 2. Fe(III) complexes of artificial and natural siderophores used in this study.

Experimental section

General

Reagents and solvents were purchased from commercial suppliers and used without further purification. All artificial siderophores and their Fe(III) complexes were prepared via previously reported methods [23–25]. All measurements were carried out at room temperature (25 °C) unless otherwise noted. Cyclic voltammograms were taken with a BIOANALYTICAL Systems model CV-1B-120. Measurements of the UV–vis spectra were performed with a JASCO U-best 560 spectrophotometer.

Electrochemistry

Cyclic voltammograms of the Fe(III)-artificial siderophore complexes (Fe-L) were measured under the following conditions: [Fe-L] (Fe : L = 1 : 1) = 1 mM, 10 mM HEPES–NaOH buffer at pH 7, 0.1 M $NaClO_4$ as the supporting electrolyte, a glassy carbon working electrode, a saturated calomel reference electrode (SCE), a Pt wire supporting electrode, and a scan rate of 100 mV/s. Before the measurements, all sample solutions were degassed by bubbling Ar gas through them for 15 minutes. The sweep potential range was set from +600 mV to –1200 mV and from +100 mV to –800 mV *vs*. SCE for Fe(III)-TAGE and Fe(III)-TAGP, respectively. The potential sweep started from 0 mV *vs*. SCE and then swept in the negative potential direction. All the measurements were performed for 5 cycles, and the 3rd cycle data, which showed a stable wave pattern, were used. The potential values, which were measured as an SCE scale, were converted to an NHE scale by the addition of +242 mV.

UV–vis spectral measurement

Spectral changes due to the reaction of ferric siderophores with ascorbic acid as a reductant were observed via UV–vis spectroscopy. A solution containing 1 mM Fe(III)-TAGE (2 mL) or 2 mM Fe(III)-DFOB (1 mL), 10 mM 2,2'-bipyridine (Bpy) (2 mL), 20 mM ascorbic acid (0 or 1 mL), and 1 M $NaClO_4$ (1 mL) containing 0.1 M Tris buffer (pH 7.4) was added to a 10 ml volumetric flask. The solution was then brought to 10 mL with water. Each final concentration was as follows: Fe(III)-TAGE or Fe(III)-DFOB = 0.2 mM, Bpy = 2 mM, ascorbic acid = 0 or 2 mM, $NaClO_4$ = 0.1 M, and Tris buffer = 0.01 M. After that, an aliquot of the solution was immediately transferred to an optical cell (cell length of 1 cm), and the absorbance was measured by a spectrometer over time.

Biological activity

M. flavescens (ATCC No. 25091) was purchased from American Type Culture Collection (ATCC). The siderophore-free ATCC No. 424 broth was prepared via the following method: 1 g of Bacto peptone, 1 g of yeast extract and 0.2 g of K_2HPO_4 were dissolved in 100 mL of water, the solution was adjusted to pH 7.4 with 1 M NaOH, and the medium was autoclaved for sterilization. Borosilicate glass test tubes (15 mL) were filled with 5 mL of siderophore-free ATCC No. 424 broth. The artificial (TAGE and TAGP) and natural (DFC and DFOB) siderophores and the other chelating agents (EDTA, Tiron, citric acid, AHA) were added to 100 μM stock solution to achieve a final concentration of 1 μM. Then, each tube was inoculated with 5 mL of the cells, incubated for two days in a platinum loop and shaken at an inclined position at 30 °C and 100 rpm. In the case of the presence of Bpy, the experimental method was identical to that used in the absence of bpy except for the use of the

corresponding iron(III) complexes (Fe(III)-TAGE, Fe(III)-TAGP, Fe(III)-DFC, and Fe(III)-DFOB) instead of their iron-free siderophores. The concentration dependence of TAGE was investigated via the same procedure by changing the final concentration of TAGE to 5, 1, 0.5, or 0.1 μM.

The growth of *M. flavescens* over time was measured as follows: borosilicate glass test tubes (5 mL) were filled with 4 mL of siderophore-free ATCC No. 424 broth. The ferric artificial or natural siderophore complexes were added to 100 μM stock solutions to achieve a final concentration of 1 mM, and then each tube was inoculated with 5 mL of the cells incubated for two days via a platinum loop. The test tubes were equipped with an ADVANTEC TN-1506 Bio-Photorecorder and shaken in an inclined position at 30 °C and 70 rpm. The optical density (O.D.) of each sample was monitored at 660 nm every 10 minutes. Another biological activity in the presence of an Fe(II) chelator (Bpy) was also examined in siderophore-free ATCC No. 424 broth containing 400 μM Bpy as a ferrous ion chelator. The experimental method was identical to that used in the absence of Bpy except for the use of the corresponding iron(III)-siderophore complexes instead of their iron-free siderophores.

Results and Discussion

Electrochemical properties

The redox potentials of the Fe(III) complexes of the artificial hydroxamate-type siderophores Fe(III)-TAGE and Fe(III)-TAGP were measured at pH 7 *via* cyclic voltammetry (CV). Although we previously reported the CV curve of the Fe(III)-TAGE complex, we remeasured it again to compare it with that of Fe(III)-TAGP under the same conditions. Their voltammograms, as shown in Fig. 1, were found to be quasireversible one-electron redox waves. The electrochemical potential values are listed in Table 1. The $E_{1/2}$ values for Fe(III)-TAGE and Fe(III)-TAGP are –227 and –268 mV *vs*. NHE, respectively, which are approximately 150~250 mV higher than those of the Fe(III)-natural siderophore complexes, Fe(III)-DFC ($E_{1/2}$ = –392 mV *vs*. NHE) and Fe(III)-DFOB ($E_{1/2}$ = –482 mV *vs*. NHE) [26,27]. Next, using the Nernst equation ($E_{1/2}$(complex) = $E_{1/2}$(Fe(III)/(II)) –59.15 log(β^{III}/β^{II}), we attempted to calculate the stability constants for the reduced species, Fe(II)-TAGE and Fe(II)-TAGP, on the basis of the potential of the Fe(III)/(II) redox pairs ($E_{1/2}$ = –732 mV *vs*. NHE) [27] and the stability constants for the oxidized species, Fe(III)-TAGE (log β^{III} = 28.7) [23] and Fe(III)-TAGP (log β^{III} = 30.6) [25]. The values of log β^{II} for Fe(II)-TAGE and Fe(II)-TAGP were calculated to be 12.5 and 13.7, respectively, which are significantly higher than those of natural siderophores (log β^{II} = 10.1 and 10.0 for Fe(III)-DFC and Fe(III)-DFOB, respectively), indicating that the artificial complexes are stable and have higher redox potentials. Furthermore, these findings indicate that Fe(III)-TAGE and Fe(III)-TAGP are more reducible than are the Fe(III) complexes of natural siderophores. The high redox potentials of these artificial siderophore Fe(III) complexes are thought to be caused by interactions that stabilize the Fe(II) form, such as intramolecular hydrogen

bonding networks or electrostatic interactions between protonated amines and hydroxamate anions, as previously elucidated by single-crystal structure analyses [23, 25]. These findings suggest that, as described below, by utilizing the electrochemical properties of Fe(III)-TAGE and Fe(III)-TAGP and their easy reducibility (high reduction potential), it may be possible to identify an alternative iron transport pathway in *M. flavescens*.

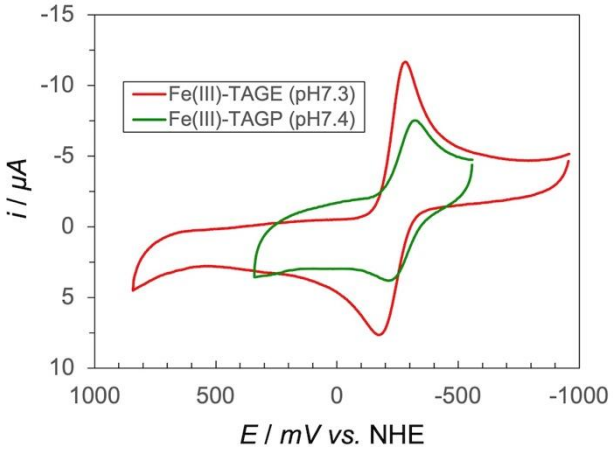


Fig. 1. Cyclic voltammograms of Fe(III)-artificial siderophore complexes, Fe(III)-TAGE and Fe(III)-TAGP, at pH 7. The sweep potential range was set from +600 mV to –1200 mV and from +100 mV to –800 mV *vs*. SCE for Fe(III)-TAGE and Fe(III)-TAGP, respectively. The potential values in the graphs are converted to an NHE scale by the addition of +242 mV.

Reduction of the Artificial Siderophore Fe(III) Complex with Ascorbic Acid as a Reductive Enzyme Model

On the basis of the experimental results described above, we suggest that we might be able to identify an alternative iron transport pathway (e.g., Path II) in *M. flavescens.* This is because Fe(III)-TAGE and Fe(III)-TAGP have high redox potentials and are therefore easily reduced; if reductases or similar enzymes are present on the cell surface, they might reduce these complexes. If reductases are present on the cell surface, reducing the Fe(III) complexes to the Fe(II) species, and if this Fe(II) species is subsequently trapped by some mechanism, bacterial growth should be inhibited. Here, we introduced 2,2'-bilyridine (Bpy) as an Fe(II) chelating agent. Bpy binds preferentially to Fe(II) ions to form a stable complex, and it is often used to demonstrate the occurrence of reductive iron transport processes such as Path II. Therefore, to investigate whether the reduced Fe(II) species is scavenged by Bpy when the artificial siderophore Fe(III) complex is reduced, we decided to study its behavior in the presence of ascorbic acid as an external reducing agent. Wirgau *et al.* [30] reported the reduction of the Fe(III)-DFOB to the Fe(II) species in the presence of Bpy using ascorbic acid ($HAsc^{\bullet -}$; the NHE potential of the $H^+/HAsc^-$ system is +282 mV) [31,32], a known biological reducing agent, and this study follows that approach. We attempted to release iron upon reduction with ascorbic acid via the Fe(III)-TAGE complex. Therefore, we tracked the changes in the UV–vis spectra of Fe(III)-TAGEs after the addition of ascorbic acid at pH 7.4 in the presence of Bpy. Figure 2A shows the time-dependent

changes in the absorption spectra of Fe(III)-TAGE upon addition of ascorbic acid in the presence of Bpy. As predicted by the stability constants between Fe(III) complexes with TAGE and Bpy (the stability constant (log β^{III} = 12.4) of $[Fe^{III}(Bpy)_3]^{3+}$ is estimated from the stability constant (log β^{II} = 17.45) [33] and redox potential ($E_{1/2}$ = 1.06 V *vs*. NHE) [34] of $[Fe^{II}(Bpy)_3]^{2+}$ according to the literature [27]), no spectral change was observed even one day after mixing Fe(III)-TAGE and Bpy without ascorbic acid (pink and blue lines in Fig. 2A). This finding indicates that the ligand exchange reaction does not occur. Furthermore, immediately after the addition of ascorbic acid, characteristic absorption bands corresponding to $[Fe^{II}(Bpy)_3]^{2+}$ appeared near 350 nm and 520 nm, indicating that the released iron was captured by Bpy. However, the one-electron redox potential of the ascorbic acid monoanion is significantly more positive than that of Fe(III)-TAGE. Wirgau *et al*. demonstrated that this is due to the formation of a ternary complex between the siderophore Fe(III) complex and Bpy [30].

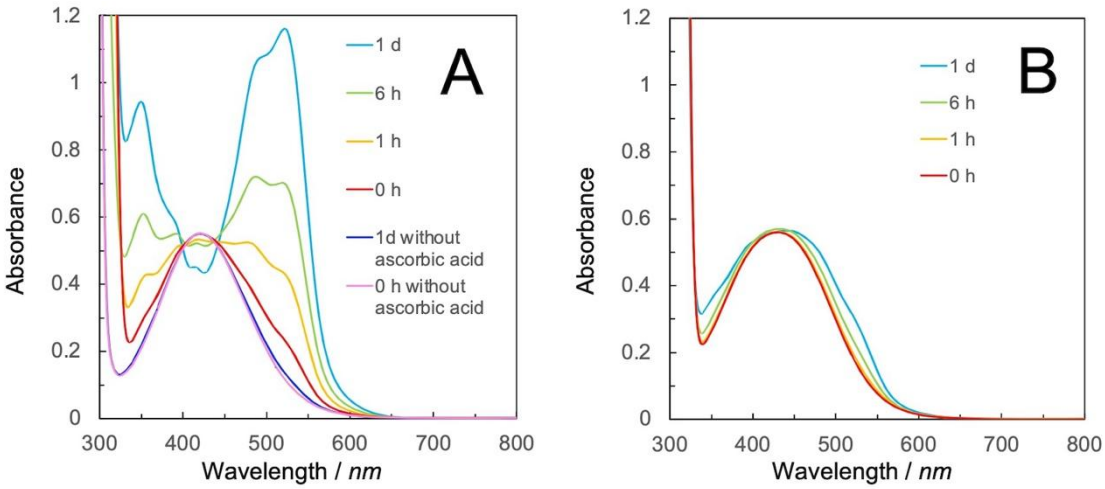


Fig. 2. UV–vis spectra of the reaction of Fe(III)-siderophores with Bpy in the presence and absence of ascorbic acid: (A) Fe(III)-TAGE and (B) Fe(III)-DFOB. Conditions: [Fe complex] = 0.2 mM, [Bpy] = 2 mM, [ascorbic acid] = 2 mM, ionic strength = 0.1 M $NaClO_4$, buffer = 0.01 M Tris buffer (pH 7.4), cell length = 10 mm, and temperature = 293 K.

On the other hand, Fe(III)-DFOB, which possesses a substantially greater negative reduction potential than does Fe(III)-TAGE (Table 1), showed almost no spectral changes under the same experimental conditions (Fig. 2B). These results indicate that Fe(III)-TAGE is readily reduced by relatively weak reducing agents such as ascorbic acid, releasing Fe(II) ions. Furthermore, our collaborators recently reported that Fe(III)-TAGEs supply iron to rice *via* a reductive iron uptake system such as Path II [35]. These findings indicate that Fe(III)-TAGE is reduced on the surface of rice roots and takes up iron into the interior of the plant. This result also suggests that *M. flavescens* can take up iron from Fe(III)-TAGE *via* the reductive iron uptake system Path II.

Growth Promotion of *M. flavescens* via Artificial Siderophores

First, we investigated the concentration-dependent effects of siderophores on the growth of *M. flavescens* via the artificial siderophore TAGE. As shown in Fig. 3, when TAGE was absent, as predicted, no growth of *M. flavescens* was observed despite the presence of sufficient iron in the culture medium. However, in the presence of 0.1 μM TAGE, slight but significant turbidity was observed, clearly indicating the growth of *M. flavescens.* Furthermore, at TAGE concentrations of 1 μM and 5 μM, the growth-promoting effects were nearly equivalent. These results demonstrate that even at a low concentration of 0.1 μM, TAGE chelates iron in the culture medium, forms Fe(III) complexes, and is taken up by *M. flavescens*. At this concentration, TAGP, another artificial siderophore, as well as the natural siderophores DFC and DFOB, also promoted the growth of *M. flavescens* (Fig. 4). Therefore, we determined that the optimal concentration of siderophores for this study was 1 μM. In contrast, other typical chelating agents, such as EDTA ($(HOOCCH_2)_2NCH_2CH_2N(CH_2COOH)_2$), Tiron ($C_6H_2(OH)_2(SO_3Na)_2$), citric acid ($HOOCC(OH)(CH_2COOH)_2$), and acetohydroxamic acid (AHA), were also investigated, but none of them promoted the growth of *M. flavescens* (Fig. 5). These findings clearly demonstrate that the artificial siderophores TAGE and TAGP, as well as natural siderophores, can capture iron ions from the culture medium and transport iron into the cells.

As described above, simple Fe(III) complexes have a higher redox potential than do Fe(III)-TAGE and Fe(III)-TAGP; for example, Fe(III)-EDTA (~ –0.2 V) [36] and Fe(III)-citrate (~ 0.0 V) [36] complexes do not promote the growth of *M. flavescens* (Figure 4). On the other hand, in plants, Fe(III)-EDTA and Fe(III)-citrate are readily available to take up iron *via* the reductive iron uptake system and promote plant growth [37,38]. Since gram-positive bacteria have a cell wall composed of peptidoglycans and negatively charged teichoic acids [39], negatively charged Fe(III) complexes such as Fe(III)-EDTA and Fe(III)-citrate may not reach the surface of the cell membrane of *M. flavescens*.

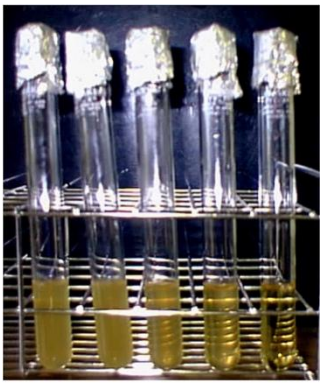


Fig. 3. Concentration dependence of the ability of TAGE to promote the growth of *M. flavescens* after 3 days of cultivation: (A) 5 μM, (B) 1 μM, (C) 0.5 μM, (D) 0.1 μM, and (E) no ligand.

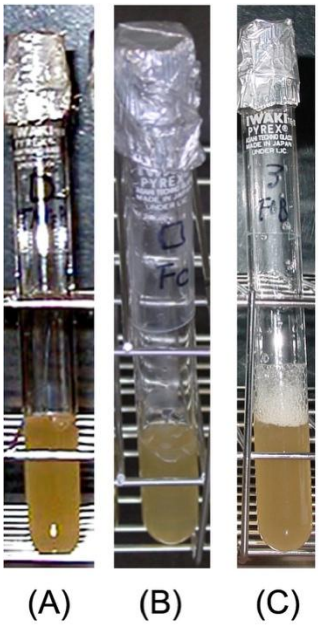


Fig. 4. Growth behavior of *M. flavescens* in liquid media after 3 days of cultivation in the presence of several siderophores: (A) TAGP, (B) DFC and (C) DFOB. The concentration of siderophores used was adjusted to 1 μM.



Fig. 5. Growth behavior of *M. flavescens* in liquid media after 3 days of cultivation in the presence of well-known chelating agents: (A) EDTA, (B) citric acid, (C) AHA, and (D) Tiron. The concentration of chelators used was adjusted to 1 μM.

Furthermore, the time course of the growth of *M. flavescens* in the presence of two artificial siderophores (TAGE and TAGP) was tracked by observing the optical density (O.D.) of the light at 660 nm via spectrophotometry. The experiment was conducted in the presence of siderophores (1 μM) under liquid culture conditions (buffer = 0.01 M Tris buffer (pH 7.4), cell length = 10 mm, temperature = 293 K). As shown in Fig. 6, both TAGE and TAGP, as well as the natural siderophore DFC, clearly presented almost the same growth curves. On the other hand, no growth of *M. flavescens* was observed in the absence

of siderophore ligands. This result suggests that the biological activities of artificial siderophores, TAGE and TAGP, are equivalent to those of natural siderophores.

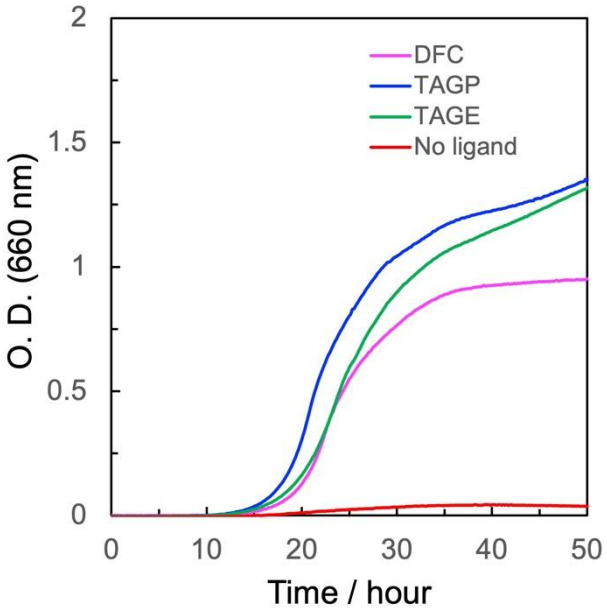


Fig. 6. Growth curves of *M. flavescens* based on spectrophotometric turbidity measurements in the presence and absence of artificial (TAGE and TAGP) and natural (DFC) siderophores. The concentration of siderophores used was adjusted to 1 μM.

Growth Promotion of *M. flavescens* via Artificial Siderophores in the Presence of 2,2'-Bipyridine

Next, we studied the growth behavior of *M. flavescens* via artificial siderophores complexed with Fe(III) in the presence of Bpy (400 μM) to determine whether *M. flavescens* undergoes a reductive iron transport process *via* Path II because Bpy is well known as an effective Fe(II) chelator and is often used to prevent iron uptake *via* Path II [17, 40–42]. Therefore, when artificial siderophore Fe(III) complexes are reduced to Fe(II) species by reductases on the cell surface, the resulting Fe(II) ions are released because of their low affinity for artificial siderophores containing hydroxamic acid groups. The released Fe(II) ions are captured by Bpy, thereby inhibiting bacterial growth *via* Path II [17, 40–42]. In contrast, iron ion uptake *via* Path I is not affected by Bpy. This is because the Fe(III) siderophore complexes taken up *via* Path I are reduced within the cell after being internalized [4]. The results of the growth behaviors of Fe(III)-TAGE and Fe(III)-TAGP are shown in Fig. 7, along with the results for the natural siderophores Fe(III)-DFC and Fe(III)-DFOB, as well as the results for the case where no Fe(III) siderophores are present (no Fe(III) complex).

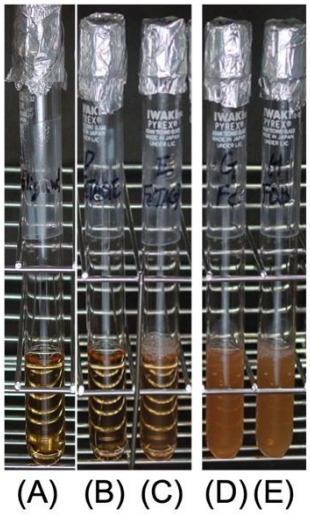


Fig. 7. Growth behaviors of *M. flavescens* in liquid medium containing Bpy (400 μM) after 6 days of cultivation in the presence or absence of several Fe(III)-siderophore complexes: (A) no Fe(III) complex, (B) Fe(III)-TAGE, (C) Fe(III)-TAGP, (D) Fe(III)-DFC, and (E) Fe(III)-DFOB. The concentration of the Fe(III) complexes was adjusted to 1 μM.

All the samples were pale red in color due to the complexation of Bpy with iron ions in the culture medium. Nevertheless, turbidity with the growth of *M. flavescens* was observed in the presence of ferric natural siderophore complexes, Fe(III)-DFC and Fe(III)-DFOB. This is because Fe(III)-DFC (log β^{III} = 29.1) [4] and Fe(III)-DFOB (log β^{III} = 30.6) [27] are more stable than $[Fe^{III}(Bpy)_3]^{3+}$ (log β^{III} = 12.4), as described above. In addition, they have more negative redox potentials (–392 mV *vs.* NHE for Fe(III)-DFC and –468 mV *vs*. NHE for Fe(III)-DFOB). Thus, these results indicate that Fe(III)-DFC and Fe(III)-DFOB are taken up into the interior of *M. flavescens via* Path I without being inhibited by the ligand exchange reaction and the reduction of the Fe(III) complexes on the cell surface. In addition, these results indicate that Bpy is not toxic to *M. flavescens.*

In contrast, in Fe(III)-TAGE and Fe(III)-TAGP, no or very little growth of *M. flavescens* was observed. When the time course of the growth of *M. flavescens* in the presence of Bpy was investigated, when Fe(III)-TAGP was used, the growth was very slow (Fig. 8). Furthermore, in the case of Fe(III)-TAGE, there was no growth of *M. flavescens* even after 10 days of cultivation. The stability constants for Fe(III)-TAGE (log β^{III} = 28.7) and Fe(III)-TAGP (log β^{III} = 30.6) are significantly greater than that of $[Fe^{III}(Bpy)_3]^{3+}$. Therefore, the inhibition of *M. flavescens* growth observed in Fe(III)-TAGE and Fe(III)-TAGP in the presence of Bpy is clearly not due to a ligand exchange reaction between these artificial siderophores and Bpy. In addition, since the culture conditions for *M. flavescens* are approximately pH 7, both artificial siderophores are stable within this pH range [24,25], and degradation of the Fe(III) complexes under these pH conditions does not seem to be a concern. Thus, this unique growth-promoting effect observed for Fe(III)-TAGE and Fe(III)-TAGP is thought to be due to differences in their electrochemical properties. This occurred because the arrest of *M. flavescens* growth in the presence of Bpy indicates that iron is in the Fe(II) state and has been

captured by Bpy. That is, the reduction potentials of Fe(III)-TAGE and Fe(III)-TAGP relative to NHE are –267 mV and –318 mV, respectively; the abnormal growth behavior of *M. flavescens* observed when Fe(III)-TAGP was used (Fig. 8) is thought to be attributable to this intermediate value of −318 mV. The above findings may suggest that, in the case of Fe(III)-TAGE and Fe(III)-TAGP, which have higher reduction potentials than ferric natural siderophore complexes do, a reductase (or reducing agent) present on the cell surface of *M. flavescens* reduces Fe(III) to Fe(II) species, and the reduced Fe(II) is captured by Bpy. This is thought to prevent Fe(II) from crossing the cell membrane, thereby inhibiting proliferation. In other words, although the specific reductase or reducing agent remains unknown, this finding suggests that Path II is present in *M. flavescens*. Table 1 summarizes the proliferation-promoting activity, stability constants, and electrochemical properties of the complexes used.

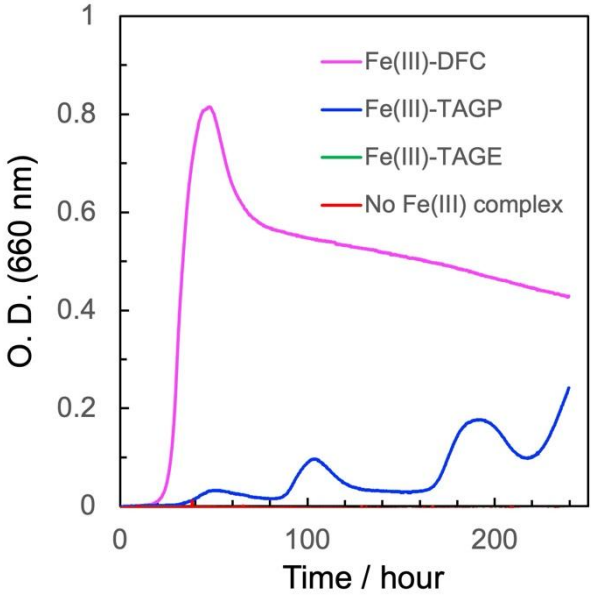


Fig. 8. Growth curves of *M. flavescens* based on spectrophotometric turbidity measurements in the presence and absence of Fe(III) complexes of artificial siderophores (Fe(III)-TAGE and Fe(III)-TAGP) (1 μM) and the natural siderophore (Fe(III)-DFC) (1 μM) in the presence of Bpy (400 μM). The measurement results for Fe(III)-TAGE and no Fe(III) complex overlap with the baseline.

Table 1. Growth-promoting activities and electrochemical properties of Fe^{III}-siderophore complexes.

	Growth-promotion activity without Bpy [a]	Growth-promotion activity with Bpy [a]	Stability constant for Fe(III) complex (log β^{III})	Stability constant for Fe(II) complex (log β^{II}) [b]	$E_{1/2}$ (mV *vs* NHE) [c]	E_{pc} (mV *vs* NHE) [c,d]	E_{pa} (mV *vs* NHE) [c,e]
Fe(III)-TAGE	++	–	28.7 [f]	12.5	–227 (–230) [f]	–283	–172
Fe(III)-TAGP	++	+	30.6 [g]	13.7	–268	–323	–213
Fe(III)-DFC	++	++	29.1[h]	10.1	–392 [i]	–426 [i,j]	–358 [i,j]
Fe(III)-DFOB	++	++	30.6 [k]	10.0 [k]	–482 [k]	–523 [j,k]	–441[j,k]

[a] ++: Strong growth, +: Faint growth, –: No growth. [b] Value estimated from the stability constant and the redox potential of the Fe(III) complex. [c] At pH 7. [d] Cathodic peak potential. [e] Anodic peak potential. [f] Ref. 23. [g] Ref. 25. [h] Ref. 4. [i] Ref. 26. [j] The values calculated from the redox potential and peak separation. [k] Ref. 27.

Conclusion

M. flavescens (ATCC No. 25091), a siderophore-dependent gram-positive bacterium, was previously thought to possess only the Path I uptake pathway, which utilizes Fe(III)-hydroxamate-type siderophores as its iron uptake system. On the basis of *in vivo* and *in vitro* experiments using Fe(III)-TAGE and Fe(III)-TAGP, artificial siderophore complexes that are highly stable and readily reduced, we discovered that *M. flavescens* also possesses a reductive iron uptake pathway (Path II). Although the detailed mechanism has not yet been elucidated, we consider ourselves very fortunate in that these findings from coordination chemistry research have led to the discovery of siderophores and genes associated with the reductive iron uptake system in *M. flavescens*.

Acknowledgments We acknowledge the Japan Society for the Promotion of Science (JSPS) for a Grant-in Aid for Challenging Research Exploratory Research (24K21786). We would like to express our gratitude to Dr. K. Jitsukawa for his helpful advice.

Author contributions All authors discussed and contributed to the final manuscript. KM: Experiments, methodology, data collection, preparation of figures and writing of the original draft, TO: Conceptualization, methodology, supervision and

editing of the original draft, TI: Conceptualization, methodology, supervision and editing of the original draft, HM: Conceptualization, methodology, supervision, preparation of figures and editing of the original draft.

Funding. Funding from JSPS, Japan, for a Grant-in Aid for Challenging Research Exploratory Research (24K21786).

Data availability. No datasets were generated or analysed during the current study.

Declarations.

Conflict of interest. The authors declare no competing interests.

Ethical approval and consent to participate. Not applicable.

Consent for publication. Not applicable.

References

1. Neilands JB (1984) In: Clarke MJ, Goodenough JB, Ibers JA, Jørgensen CK, Mingos DMP, Neilands JB, Palmer GA, Reinen D, Sadler PJ, Weiss R, Williams RJP (eds) Structure and Bonding, Vol. 58: Siderophores from Microorganisms and Plants. Springer-Verlag, Berlin, pp 1–24.
2. Hider RC (1984) In: Clarke MJ, Goodenough JB, Ibers JA, Jørgensen CK, Mingos DMP, Neilands JB, Palmer GA, Reinen D, Sadler PJ, Weiss R, Williams RJP (eds) Structure and Bonding, Vol. 58: Siderophores from Microorganisms and Plants. Springer-Verlag, Berlin, pp 25–87.
3. Sugiura Y, Nomoto K (1984) In: Clarke MJ, Goodenough JB, Ibers JA, Jørgensen CK, Mingos DMP, Neilands JB, Palmer GA, Reinen D, Sadler PJ, Weiss R, Williams RJP (eds) Structure and Bonding, Vol. 58: Siderophores from Microorganisms and Plants. Springer-Verlag, Berlin, pp 107–135.
4. Hider RC, Kong X (2010) Chemistry and biology of siderophores. Nat Prod Rep 27:637–657. https://doi.org/10.1039/b906679a
5. Sandy M, Butler A (2009) Microbial Iron Acquisition: Marine and Terrestrial Siderophores. Chem Rev 109:4580–4595. https://doi.org/10.1021/cr9002787
6. Krewulak KD, Vogel HJ (2008) Structural biology of bacterial iron uptake. Biochim Biophys Acta 1778:1781–1804. https://doi.org/10.1016/j.bbamem.2007.07.026
7. Matzanke BF, Müller-Matzanke G, Raymond KN (1989) In: Loehr TM (ed) Physical Bioinorganic Chemistry, Vol. 5: Iron Carriers and Iron Proteins. VCH, New York, pp 1–121.
8. Braun V, Hantke K, Köster W (1998) In: Sigel A, Sigel H (eds) Metal Ions in Biological Systems, Vol. 35: Iron transport and storage in microorganisms, plants, and animals. Marcel Dekker, New York, pp 67–145.
9. Mori S (1998) In: Sigel A, Sigel H (eds) Metal Ions in Biological Systems, Vol. 35: Iron transport and storage in microorganisms, plants, and animals. Marcel Dekker, New York, pp 215–238.
10. Aisen P (1998) In: Sigel A, Sigel H (eds) Metal Ions in Biological Systems, Vol. 35: Iron transport and storage in microorganisms, plants, and animals. Marcel Dekker, New York, pp 585–631.
11. Morrissey J, Guerinot ML (2009) Iron Uptake and Transport in Plants: The Good, the Bad, and the Ionome. Chem Rev 109:4553–4567. https://doi.org/10.1021/cr900112r

12. Oka N, Sumida T, Hiraoka M, Ohno M (2008) Effects of Fe(II) for tank cultivation of Ulva prolifera in deep seawater. Algal Resources 1:63–66. https://doi.org/10.20804/jsap.1.2_63

13. Ishimaru Y, Suzuki M, Tsukamoto T, Suzuki K, Nakazono M, Kobayashi T, Wada Y, Watanabe S, Matsuhashi S, Takahashi M, Nakanishi H, Mori S, Nishizawa NK (2006) Rice plants take up iron as an Fe^{3+}-phytosiderophore and as Fe^{2+}. Plant J 45:335–346. https://doi.org/10.1111/j.1365-313X.2005.02624.x

14. Fischbach MA, Lin H, Liu DR, Walsh CT (2006) How pathogenic bacteria evade mammalian sabotage in the battle for iron. Nat Chem Biol 2:132–138. https://doi.org/10.1038/nchembio771

15. Philpott CC (2006) Iron uptake in fungi: A system for every source. Biochim Biophys Acta 1763:636–645. https://doi.org/10.1016/j.bbamcr.2006.05.008

16. Wyckoff EE, Mey AR, Leimbach A, Fisher CF, Payne SM (2006) Characterization of Ferric and Ferrous Iron Transport Systems in Vibrio cholerae. J Bacteriol 188:6515–6523. https://doi.org/10.1128/JB.00626-06

17. Yun C-W, Bauler M, Moore RE, Klebba PE, Philpott CC (2001) The Role of the FRE Family of Plasma Membrane Reductases in the Uptake of Siderophore-Iron in Saccharomyces cerevisiae. J Biol Chem 276:10218–10223. https://doi.org/10.1074/jbc.M010065200

18. Sheldon JR, Laakso HA, Heinrichs DE (2016) Iron Acquisition Strategies of Bacterial Pathogens. Microbiol Spectrum 4:VMBF-0010-2015. https://doi.org/10.1128/microbiolspec.VMBF-0010-2015

19. Sheldon JR, Heinrichs DE (2015) Recent developments in understanding the iron acquisition strategies of gram positive pathogens. FEMS Microbiol Rev 39:592–630. https://doi.org/10.1093/femsre/fuv009

20. Fukushima T, Benjamin EA, Raymond KN (2014) Direct Evidence of Iron Uptake by the Gram-Positive Siderophore-Shuttle Mechanism without Iron Reduction. ACS Chem Biol 9:2092–2100. https://doi.org/10.1021/cb500319n

21. Miethke M, Monteferrante CG, Marahiel MA, van Dijl JM (2013) The Bacillus subtilis EfeUOB transporter is essential for high-affinity acquisition of ferrous and ferric iron. Biochim Biophys Acta 1833:2267–2278. https://doi.org/10.1016/j.bbamcr.2013.05.027

22. Trindade IB, Fonseca BM, Catarino T, Matias PM, Moe E, Louro RO (2025) Flavin-containing siderophore-interacting protein of *Shewanella putrefaciens* DSM 9451 reveals common structural and functional aspects of ferric–siderophore reduction. J Biol Inorg Chem 30:241–255. https://doi.org/10.1007/s00775-025-02106-z

23. Matsumoto K, Ozawa T, Jitsukawa K, Einaga H, Masuda H (2001) Crystal Structure and Redox Behavior of a Novel Siderophore Model System: A Trihydroxamato-Iron(III) Complex with Intra- and Interstrand Hydrogen Bonding Networks. Inorg Chem 40:190–191. https://doi.org/10.1021/ic0007411

24. Matsumoto K, Ozawa T, Jitsukawa K, Masuda H (2004) Synthesis, Solution Behavior, Thermal Stability, and Biological Activity of an Fe(III) Complex of an Artificial Siderophore with Intramolecular Hydrogen Bonding Networks. Inorg Chem 43:8538–8546. https://doi.org/10.1021/ic048761g

25. Matsumoto K, Suzuki N, Ozawa T, Jitsukawa K, Masuda H (2001) Crystal Structure and Solution Behavior of the Iron(III) Complex of the Artificial Trihydroxamate Siderophore with a Tris(3-aminopropyl)amine Backbone. Eur J Inorg Chem 2001:2481–2484. https://doi.org/10.1002/1099-0682(200109)2001:10%3C2481::AID-EJIC2481%3E3.0.CO;2-G

26. Wawrousek EF, McArdle JV (1982) Spectroelectrochemistry of ferrioxamine B, ferrichrome, and ferrichrome A. J Inorg Biochem 17:169–183. https://doi.org/10.1016/S0162-0134(00)80097-5

27. Spasojević I, Armstrong SK, Brickman TJ, Crumbliss AL (1999) Electrochemical Behavior of the Fe(III) Complexes of the Cyclic Hydroxamate Siderophores Alcaligin and Desferrioxamine E. Inorg Chem 38:449–454. https://doi.org/10.1021/ic980635n

28. Burnham BF, Neilands JB (1961) Studies on the Metabolic Function of the Ferrichrome Compounds. J Biol Chem 236:554–559. https://doi.org/10.1016/S0021-9258(18)64402-3

29. Guerinot ML (1994) MICROBIAL IRON TRANSPORT. Annu Rev Microbiol 48:743–772. https://doi.org/10.1146/annurev.mi.48.100194.003523

30. Alderman BW, Ratliff AE, Wirgau JI (2009) A mechanistic study of ferrioxamine B reduction by the biological reducing agent ascorbate in the presence of an iron(II) chelator. Inorg Chim Acta 362:1787–1792. https://doi:10.1016/j.ica.2008.08.024

31. Koppenol WH, Hider RH (2019) Iron and redox cycling. Do's and don'ts. Free Radic Biol Med 133:3–10. https://doi.org/10.1016/j.freeradbiomed.2018.09.022

32. Williams NH, Yandell JK (1982) Outer-sphere electron-transfer reactions of ascorbate anions. Aust J Chem 35:1133–1144. https://doi.org/10.1071/CH9821133

33. Anderegg G (1963) Pyridinderivate als Komplexbildner V. Die Metallkomplexe von 1,10-Phenanthrolin und α, α'-Dipyridyl. Helv Chim Acta 46:2397–2410. https://doi.org/10.1002/hlca.19630460657

34. Holubowitch NE, Nguyen G (2022) Dimerization of $[Fe^{III}(bpy)_3]^{3+}$ in Aqueous Solutions: Elucidating a Mechanism Based on Historical Proposals, Electrochemical Data, and Computational Free Energy Analysis. Inorg Chem 61:9541–9556. https://doi.org/10.1021/acs.inorgchem.2c00640

35. Ueno D, Matsumoto K, Enami T, Nishiyama N, Kato S-I, Iwasaki K (2019) Efficacy of an artificial microbial siderophore-Fe(III) with high redox potential on correcting Fe chlorosis in rice. Soil Sci Plant Nutr 65:471–478. https://doi.org/10.1080/00380768.2019.1648180

36. Kosman DJ (2003) Molecular mechanisms of iron uptake in fungi. Mol Microbiol 47:1185–1197. https://doi.org/10.1046/j.1365-2958.2003.03368.x

37. Van Driel W (1964) THE EFFECT OF IRON ETHYLENEDIAMINETETRAACETIC ACID ON THE GROWTH AND METABOLISM OF TOMATO PLANTS IN WATER CULTURE. Plant Soil 20:85–104. https://doi.org/10.1007/BF01378101

38. Kobayashi T, Nishizawa NK (2012) Iron Uptake, Translocation, and Regulation in Higher Plants. Annu Rev Plant Biol 63:131–152. https://doi.org/10.1146/annurev-arplant-042811-105522

39. Swell EWC, Brown ED (2014) Taking aim at wall teichoic acid synthesis: new biology and new leads for antibiotics. J Antibiot 67:43–51. https://doi:10.1038/ja.2013.100

40. McHugh JP, Rodríguez-Quiñones F, Abdul-Tehrani H, Svistunenko DA, Poole RK, Cooper CE, Andrews SC (2003) Global Iron-dependent Gene Regulation in *Escherichia coli* A NEW MECHANISM FOR IRON HOMEOSTASIS. J Biol Chem 278:29478–29486. https://doi.org/10.1074/jbc.m303381200

41. Lakshminarayanan K, Murugan D, Venkatesan J, Thirumalaiswamy HV, Gadais C, Rangasamy L (2024) Siderophore-Conjugated Antifungals: A Strategy to Potentially Cure Fungal Infections. ACS Infect Dis 10:2448–2466. https://doi.org/10.1021/acsinfecdis.4c00046

42. Gaspar M, Santos MA, Krauter K, Winkelmann G (1999) Molecular recognition of synthetic siderophore analogues: A study with receptor-deficient and fhu(A-B) deletion mutants of Escherichia coli. BioMetals 12:209–218. https://doi.org/10.1023/A:1009218812778